13th World Conference on Earthquake Engineering
Vancouver, B.C., Canada
August 1-6, 2004
Paper No. 1808

EXPERIMENTAL RESULTS ON EARTH PRESSURES ON RIGID WALL UNDER SEISMIC CONDITION

Agatino Simone Lo Grasso[1], Michele Maugeri[2] and Ernesto Motta[3]

SUMMARY

This paper contains the experimental results of a series of shaking table tests of a model of gravity retaining wall, with the purpose to investigate the distribution of dynamic earth pressure in dry cohesionless backfill and the effects of the soil-wall friction on the distribution of pressure.
All the tests were conducted at the University of Catania shaking table. The models were instrumented to measure displacements, accelerations and dynamic pressure. The results of the experimental program show that the dynamic earth pressure distribution is influenced by the wall movement modes and the point of application of the active thrust is always near the top of the wall. The reduction of the wall friction produces an increment of dynamic pressure, influencing the failure mode of the soil-wall system. All the recorded pressure shows a non linear distribution with depth.

INTRODUCTION

The evaluation of the dynamic earth pressure is an important aspect in the retaining structures design. Recent earthquakes show that the pressure distribution depends on the wall movement and on the acceleration level; the magnitude of the total lateral earth pressure and the point of application of the total thrust are not univocally determinate and these values often differ from M&O solution. The method is based on three assumption: the wall has already deformed outwards sufficiently to generate the minimum active earth pressure; a planar failure surfaces were formed when lateral soil deformation becomes large enough to fully mobilize the shear strength of the soil; the soil wedge formed is considered as a rigid body so that the acceleration maintaining constant his value with depth and amplification effect is not observed. This theory, however, cannot take into account the effects of soil deformation and the consequent degradation of internal friction angle to residual state that occur in a dense soil during an earthquake.

[1] PhD Doctor Dept. of Civil and Environmental Engineering University of Catania, Italy, e-mail: simone.lograsso@tiscalinet.it
[2] Full Professor in Geotechnical Engineering, Dept. of Civil and Environmental Engineering University of Catania, Italy, e-mail: mmaugeri@dica.unict.it
[3] Professor in Geotechnical Engineering, Dept. of Civil and Environmental Engineering University of Catania, Italy, e-mail: emotta@dica.unict.it

Many authors have studied the distribution of the static and dynamic earth pressure, with various solutions, yet there is not enough experimental analysis to validate these theories and especially in evaluating the effects of the soil-wall friction angle on dynamic earth pressure.
Prakash (1981) reported a course study conducted by Nandakumaran [6] on rigid walls, 1 meter high, with different wall movements, showing that the distribution of pressures is non linear with depth and the maximum value is reached at 65% of wall height from the top of the wall. Sherif, Ishibashi and Lee (1982) [10] conducted a series of tests on the Washington University shaking table. The quasi-static and dynamic tests showed that the pressure distribution was dependent on the soil-wall friction angle and that the critical value of the wall displacement is:

$$S=H(7-0,13\varphi)10-4$$

where H is the height of the wall an φ is the value of internal friction angle. The tests shows that the value of dynamic pressure is increased of 30% respect the theoretical prediction and the point of application of total active thrust can be assumed to 0.45H from the base of the wall.
The distribution of the dynamic pressure is influenced by the wall movements as shown in the tests conducted by Sherif & Fang (1984) [9] where the wall is constrained to rotate about the top. In these tests was observed an increment of the pressure near the top of the wall due to arching stress effect of the soil and the point of application of total thrust corresponding to the value of 0.55H from the base of the wall. These results compare well with those computed previously by Scott (1973), Matsuo and Ohara (1960) [4] and Wood (1973) as well as by Fang and Ishibashi, (1986) [1] and Ishibashi and Fang (1987) [2]. Recent theoretical approaches have been developed to determine a more careful method of prediction of the total earth pressure under seismic conditions based on a kinematical approach (Soubra and Macuh, 2001) [11], or considering the effects of strain localization (Zhang and Li, 2001) [16], or considering the lateral deformation of the soil between the active and passive states of stress, including the state at rest (Zhang, Shamoto and Tokimatsu, 1998a, Zhang, Shamoto and Tokimatsu, 1998b, Zhang, Shamoto and Tokimatsu, 1998c) [13] [14] [15].
This paper gives an experimental confirmation to the theoretical approaches showing that the distribution of earth pressure under seismic conditions is non-linear. The point of application of the total thrust is strongly dependent by the wall movements during the motion and the distribution is also influenced by the soil-wall friction angle. The results of the tests compare well with those computed using the pseudo-dynamic approach similar to the method of Steedman and Zeng, (1990) [12] where the sinusoidal acceleration along the wall is given by

$$\ddot{u}(z,t)=k_h g sen\omega\left(t-\frac{H-z}{V_s}\right)$$

where Vs is the shear wave velocity, ω is the pulsation of the lateral shaking, H is the height of the wall and z the current height. The final expression of the distribution of the lateral pressure can be expressed as:

$$p_{AE}=\frac{\cos(\alpha-\phi)k_h\gamma z}{\cos(\delta-\alpha+\phi)\tan\alpha}sen\omega\left(t-\frac{z}{V_s}\right)+\frac{sen(\alpha-\phi)\gamma z}{\cos(\delta-\alpha+\phi)\tan\alpha}$$

which is clearly non linear.

EXPERIMENTAL PROCEDURE

The shaking table of the laboratory of the University of Catania consists in a steel frame and a steel plate bolted on the frame. It is 2 m long, 1 m wide and 80mm thick and is supported by four rollers constrained to move on rails, in order to restrict the motion only to one direction.
The test box is 1 m long, 0.70 m wide and 0.40 m. The motion is provided to the table by a loading unit consisting of a hydraulic system whose capacity is to transfer a static load of 3000 daN and a dynamic load equal to 1000 daN when the acceleration value is equal to 2g. The system is able to transfer a maximum displacement equal to ±25mm. The sides of the test box are in glass with the purpose to observe

the model deformation and the failure surface during the test. The thickness of the glass sides was chosen equal to 10mm in order to ensure a plane-strain deformation.The wall used in the tests is a model micro concrete gravity retaining wall of height H=30 cm. In order to avoid friction between the wall and the glass side of the test box, the wall was made 5mm shorter than the box width and the wall ends were equipped with flexible plastic flags to prevent sand passing through the lateral gaps. The soil used in all tests is a dry silica sand from the Sicily east coast which characteristics are D_{60}/D_{10} = 2.407, D_{50} = 0.42mm, maximum and minimum unit weight γ_{max}=18.27KN/m3 and γ_{min}=15.04 KN/m3 respectively, and peak value of the shear strength angle φ = 37° obtained at the same relative density used in the tests as a result of a series of direct shear tests.

The backfill were prepared by dry pluviation in the test box, in which the deposition height was maintained constant respect the backfill, obtaining a final relative density Dr≅75%. In each test the model was instrumented with two accelerometers and two LVDT displacement transducers with the purpose to record accelerations and displacements at the top and at the base. A further accelerometer was placed into the backfill, outside the failure wedge, to measure the soil acceleration. Five pressure transducers were fixed on the internal face of the wall; the transducers were provided of a circular contact area of 1 cm of diameter, to record the value of pressure at an interval of 6 cm along the depth. In figure 1 is shown the experimental devices. A data acquisition system and software for data processing were employed to record and analyze data obtained during dynamic testing. To observe the formation of the failure surface through the glass side of the test box, vertical black sand marchers were introduced into the backfill.

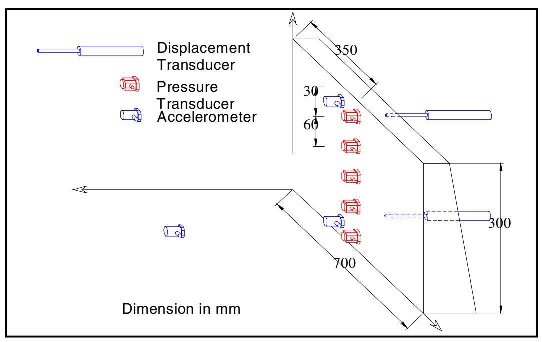

Figure 1: Position of measure instruments

RESULTS

General

The soil-wall systems were subjected to a sinusoidal input acceleration whose amplitude was strongly increased with time until to a maximum value whereas the frequency was maintained constant. A certain number of models were investigated; in this paper four tests are reported. The label "TH" indicates the models in which the soil-wall friction angle was not reduced and the label "TG" indicates the models in which the soil-wall friction angle was strongly reduced introducing a thin glass sheet that was glued on the internal face of the wall. The frequency of the input motion was fixed to the value of 6Hz, while two different values of the amplitude, equal to 2,5mm and 3,0mm, were used. These amplitude values are able to transfer to the system a maximum acceleration of 0.37g and 0.43g respectively.

Displacements and dynamic pressure analysis

Time-histories of displacements and rotation for the tests named TH4 and TG2 (f=6Hz, s=2.5mm) are shown in figure 2.

For the test TH4, the accumulation of permanent displacements was gradual, but a large vibration was possible to be observed at the top of the wall from the beginning of the shaking test. This vibration increases when the wall and the table accelerations are negative, that is, directed backward. The rotation of the system shows different wall movement modes during the same test. It is possible to distinguish a first stage (until 13 sec.) in which the top of the wall, accumulates permanent displacements and rotations, maintaining large vibrations.

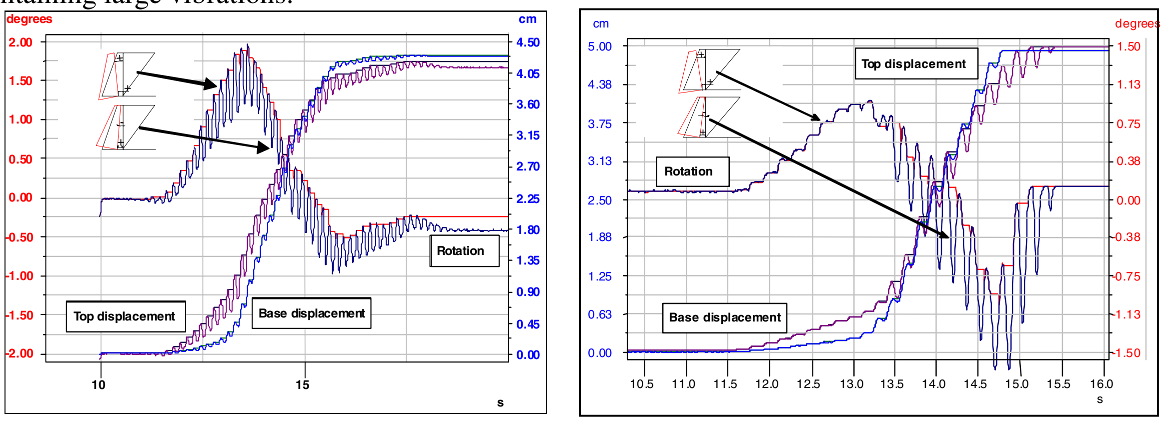

Figure 2: wall displacements and system rotation for the tests TH4 (on the left) and TG2 (on the right)

In a second stage (after 13 sec), in which, is reached the threshold acceleration value, a sudden increase of the permanent wall base displacement was observed. At this phase of the motion corresponded an abrupt change in the rate of rotation which inverts his course. These two distinct modes of system rotations produced different distributions of dynamic pressure, generating, during the second stage, “passive” phenomena between the wall and the backfill near the top. In figure 3 is shown a detail of the recorded data at the instant of the translational failure.

The notations PTh15 and PTh21, in figure 3, represent the data of the pressure transducers at 15cm and 21cm of depth respectively. Figure 3 also shows the distribution of the total dynamic pressure at the two different stages of collapse of the soil-wall system.

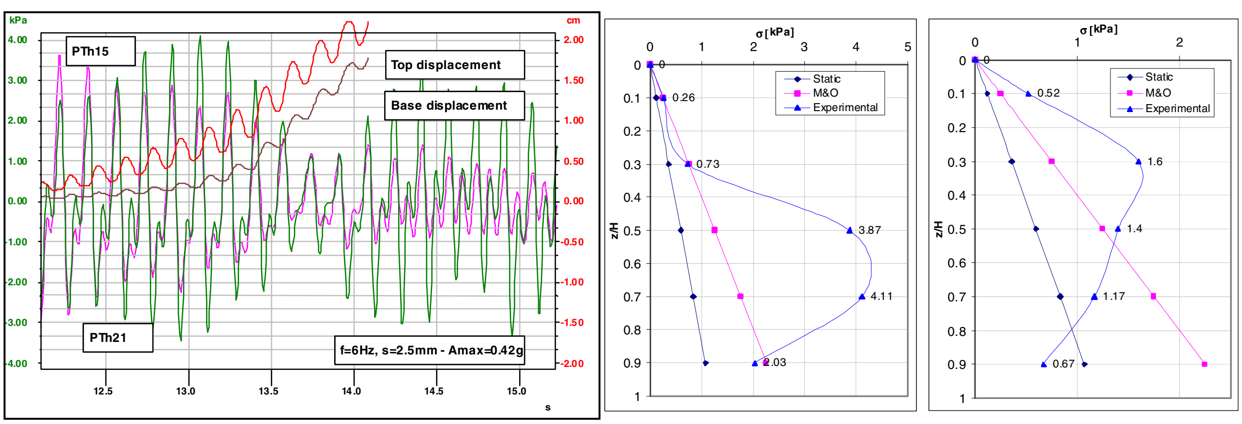

Figure 3: wall displacements and pressures for the test TH4 (on the left) and the distribution of the dynamic pressure for the test TH4 for the two different wall movement modes (on the rights)

The recorded pressures were compared with those computed with the M&O and Coulomb theories, assuming a linear distribution. From the data recorded for the test TG2 can be observed that the accumulation of permanent displacements was achieved without large vibration at the top of the wall from the beginning of the shaking test. The increase in the wall vibration is evident when the limit equilibrium at the base is reached and an evident translation of the wall appears. This different behaviour could be attributed to the reduction of the soil-wall friction angle value. Also in this test the system shows different wall movement modes.

Comparing the two tests, it can be observed that the final permanent displacements value are approximately the same, but the test TG2 shown a notable reduction of rotation both at the first stage and at the end of the shaking test.
The reduction of the soil-wall friction angle and the consequently reduction of the top wall oscillation, produced a distribution of the dynamic pressure, that is characterized by a strong value of the pressure recorded near the top of the wall, even when the limit equilibrium was reached, due to the sudden increase of permanent displacements at the base, with the consequent action of the "passive" effects between the wall and the backfill. Figure 4 shows the time-history of the pressure transducers. The notations PTh have the same previous sense of figure 3.

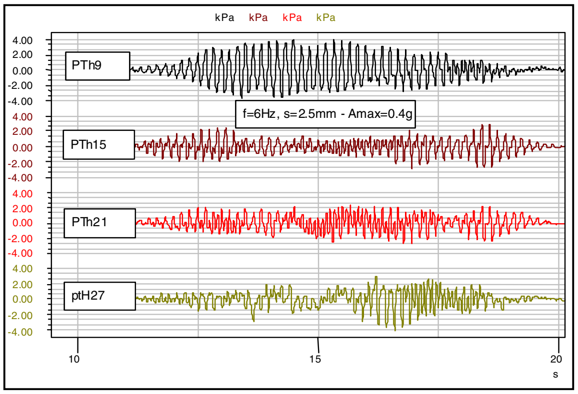

Figure 4: time-histories of the pressure transducers of the test TG2

Figure 5 shows the distribution of the total dynamic pressure at the collapse of the system. Similar results were obtained for the tests in which the shape of sinusoidal input is different and the acceleration level was increased linearly until the end of the test.

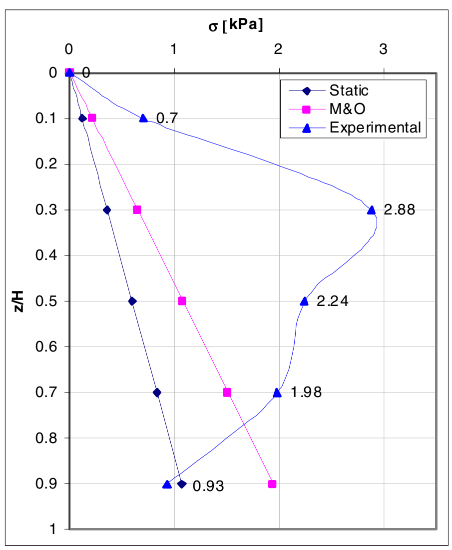

Figure 5: distribution of the dynamic pressure for the test TG2

The two tests reported in this paper, labeled TH8 and TG4, show the same behaviour of the tests previously described. Two different stages of rotation corresponding to two different distributions of dynamic pressures are evidenced: a marked oscillation of the top of the wall for the system without reduction of the soil-wall friction and an evident sudden increase of permanent displacement at the base, with the "passive" effects for the system with low soil-wall friction.

Comparing the final values of permanent displacements and rotations, it is possible to observe that the final value of displacement is the same for both tests but a reversal of the final rotation was recorded for the test with the lower soil-wall friction angle. These results are plotted in fig.6. The distributions of dynamic pressure are plotted in figure 7.

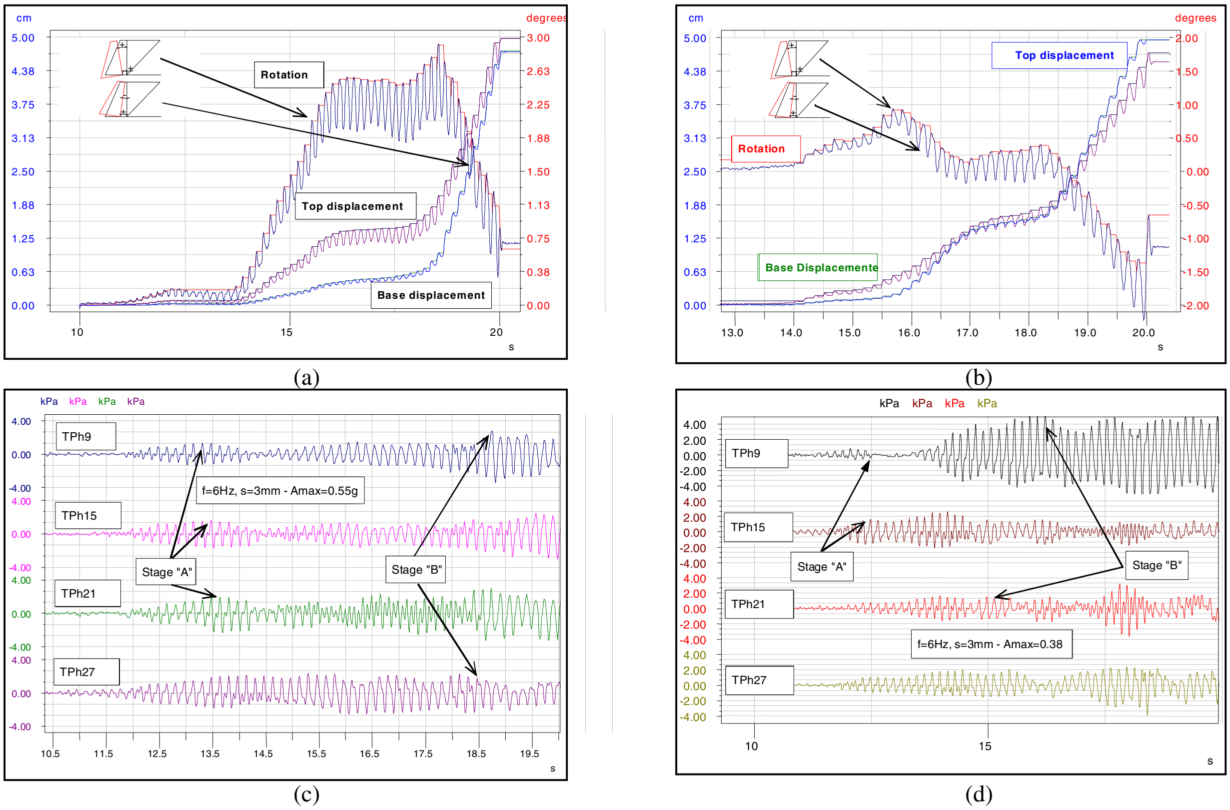

Figure 6: a) wall displacements and system rotation test TH8; (b) wall displacements and system rotation test TG4; (c) time-history of dynamic pressures test TH8; (d) time-history of dynamic pressures test TG4

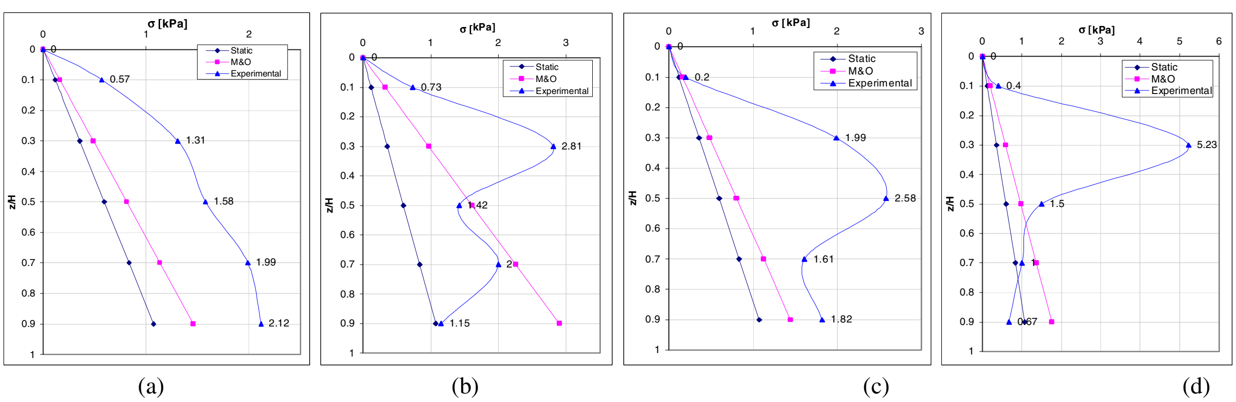

Figure 7: (a) distribution of dynamic pressure at stage "A" test TH8; (b) distribution of dynamic pressure at stage "B" test TH8; (c) distribution of dynamic pressure at stage "A" test TG4; (d) distribution of dynamic pressure at stage "B" test TG4

Base motion amplification analysis

The accelerometric data show a similar behaviour for all systems tested: before the threshold acceleration is reached, the wall acceleration is similar to the acceleration in the backfill; when input acceleration is grater than the threshold acceleration, a cutoff for the wall is clearly evident, indicating that a relative displacement has developed in the system and a series of amplification phenomena appear. Figure 8 shows the input, top and base accelerations, and relative displacements time-history for the test TH4, whereas in figure 9 the peak accelerations progress are reported. The parabolic line represents the envelope of the peaks of input acceleration. It is apparent that permanent displacements build up in the outward direction when the table is moving backward. After 13 seconds, when the input acceleration is equal to 0.32g the wall base shows a reduction of the acceleration up to 0.25g, whereas the wall top acceleration, at the same time, showed amplification phenomena when the input acceleration was 0.20g at 11.8 sec. This behaviour is more evident for the accelerations in the backward direction. When the wall base acceleration shown a reduction, a failure surface was clearly formed and observed through the glass side of the test box. At the maximum value of input acceleration was recorded an amplification of the wall top acceleration of about 50% and a reduction of wall base acceleration of about 30%.

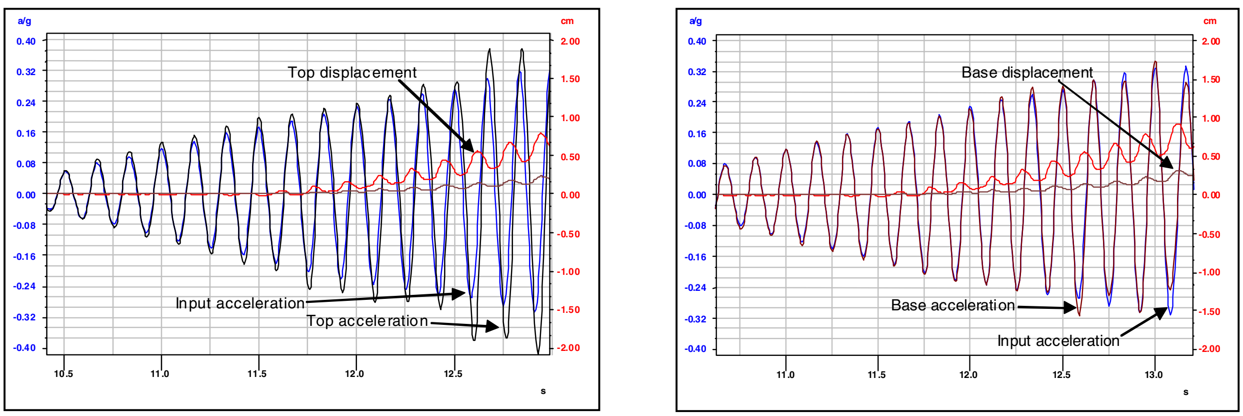

Figure 8: input and wall top acceleration compared with wall top and base displacements (on the left); input and wall base acceleration compared with wall top and base displacements (on the right)

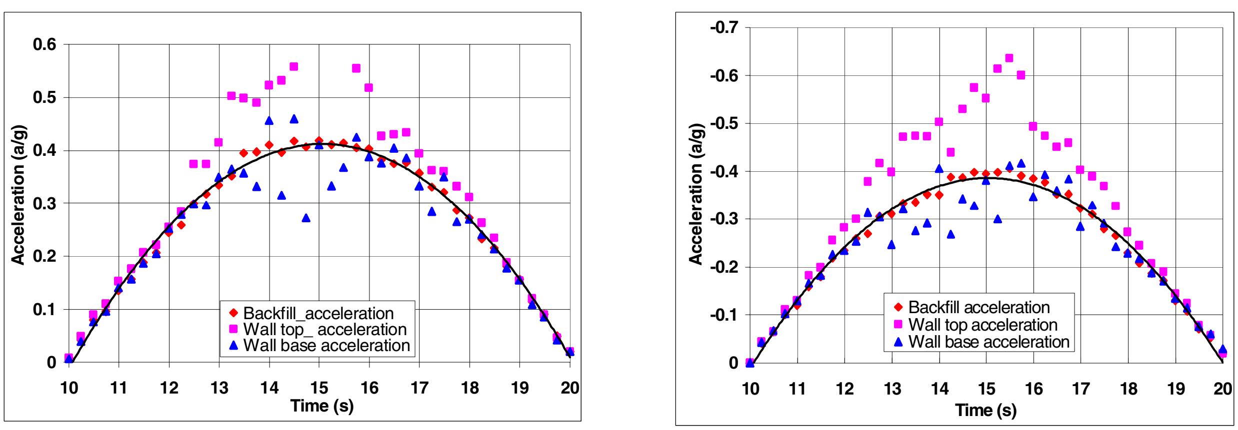

Figure 9: time-histories of peak accelerations when system was direct outward(on the left); time-histories of peak accelerations when system was direct backward (on the right)

Moreover with the amplification phenomena recorded is associated a difference of phase between the accelerometric records of the input and of the top of the wall, as shown in the previous fig.8a.This phase change in lateral acceleration plays an important role on the distribution of the dynamic increment of the earth pressure. These results compare well with those measured by Steedman and Zeng (1990) by centrifuge tests. In figure 10 the accelerations and displacements time-history as well as the peak accelerations progress for the test TG2 are reported. For the same test, after about 13 seconds, when the input acceleration is equal to 0.32g the wall base shows a reduction of the acceleration until 0.22g, whereas the wall top acceleration showed amplification phenomena when the input acceleration was 0.25g at 12 sec. This behaviour is again evident for the accelerations in the backward direction. At the maximum value of input acceleration was recorded a very strong amplification of the wall top acceleration of about 100% and a reduction of wall base acceleration, similar to the TH4 test, of about 30%. Also for this test, the amplification phenomena recorded are associated to a different of phase between the accelerometric records of input and of wall top. Similar results were obtained for the test TH8 and TG4.

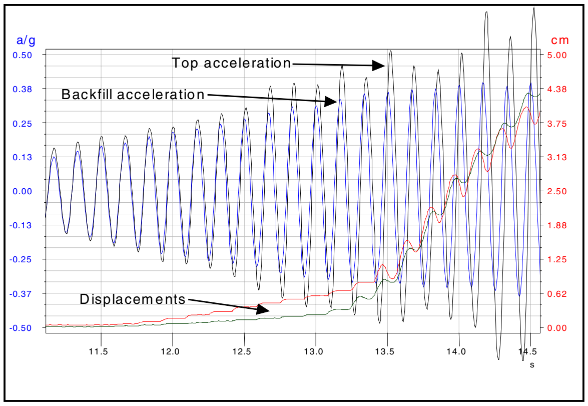

(a)

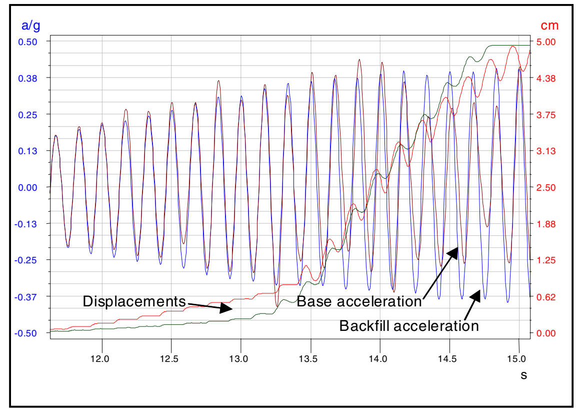

(b)

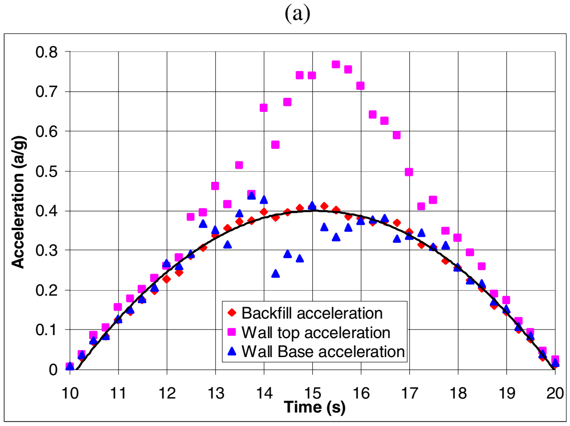

(c)

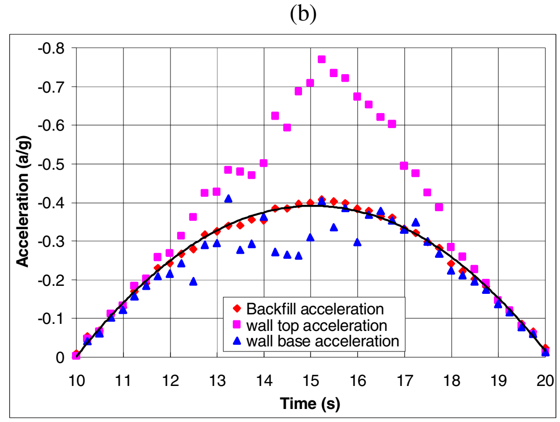

(d)

Figure 10 (a) input and wall top acceleration compared with wall top and base displacements; (b) input and wall base acceleration compared with wall top and base displacements; (c) time-histories of peak accelerations when system was direct outward; (d) time-histories of peak accelerations when system was direct backward

Failure surface analysis

For all tests a clear failure surface was observed. In figure 11 the system TH4 before and after the development of the failure surface is reported. It is clear the effectiveness of black sand markers evidencing the failure surface. An evident concavity was detected in the failure surface as remarked by the red curve. For this test the angle formed by the failure surface with the horizontal was approximately assumed equal to 55°. The rotational behaviour described previously, is emphasized by the large inclination of the black sand markers placed inside the failure wedge, whereas the failure surface is well evidenced due to the large permanent displacement of the wall. The average value of the vertical markers rotation is equal to 5° direct clockwise. When the soil-wall friction was reduced, in the test TG2, a different failure mode of the system was observed and a different failure wedge formed at the end of the test (figure 12). For this test, is clear that the failure surface is a plane, as proved by the red line, with the angle formed respect the horizontal equal to 60°. The rotational behaviour is emphasized by the large inclination of the black sand markers placed both inside the failure wedge and both especially outside the failure wedge. The average value of the vertical markers rotation is equal to 9° direct clockwise. For the test TH8 and TG4 similar results were observed and it had been reported in figure 13.

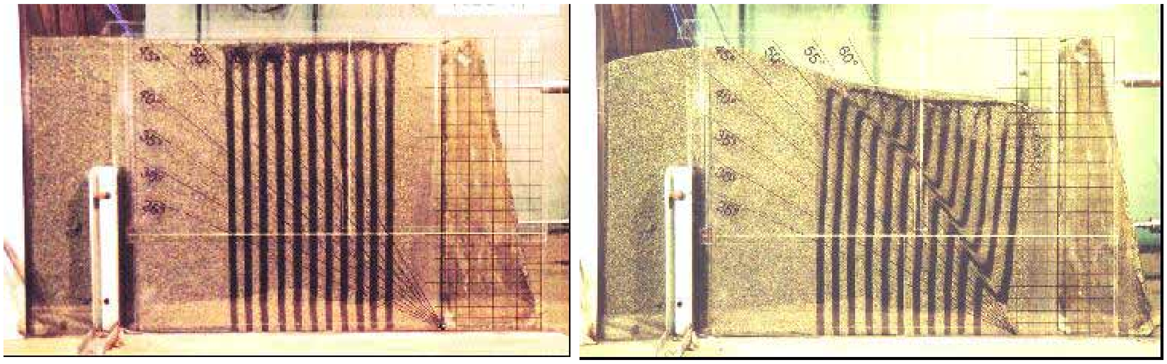

(a) (b)

Figure 11: The system named TH4: (a) before and (b) after the formation of the failure surface

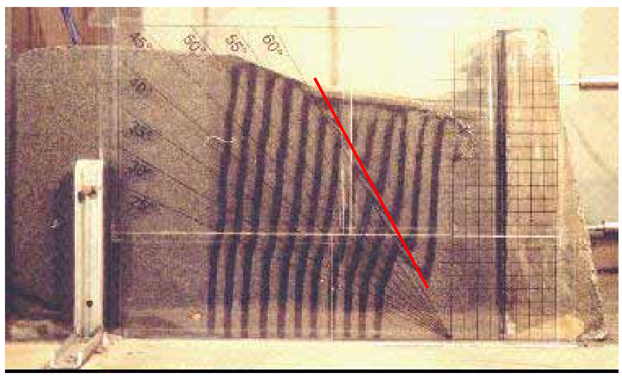

Figure 12: The system named TG2 after the formation of the failure surface

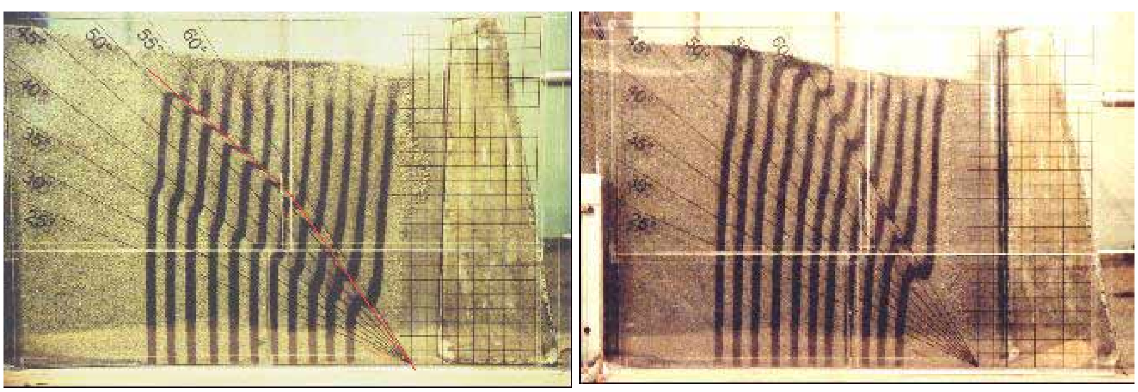

(a) (b)

Figure 13: The systems named TH8 (a) and TG4 (b) after the formation of the failure surface.

DISCUSSION

Analyzing the previous data can be underlined that a reduction of soil-wall friction angle produces a very large increment of acceleration level at the wall top. With this behaviour two different types of displacements are associated: a recoverable and an irrecoverable that occur for each cycle of input load; the first, defined as "elastic displacement" can be calculated and his effects on acceleration level can be expressed by the follow equation:

$$\ddot{s}'_w = \frac{\partial^2 (s + x_t)}{\partial t^2} = \frac{\partial^2 s}{\partial t^2} + \frac{\partial^2 x_t}{\partial t^2}$$

where "s" is the displacement imposed by the input motion and "xt" is the relative displacement between the soil-table system and the top wall. The tests conducted have shown that, the "elastic" displacement of the wall top is depending by the value of soil-wall friction angle, especially in the initial stage of the motion, and that his value has a significant influence on dynamic pressure. Displacement analysis shows that two different wall movement modes occur during the same test. In a first stage a reduction of the pressure cells TPh3 and TPh9, because of the initial rotation and to a strong increment of the dynamic earth pressure near the base was observed, with the maximum value recorded at the load cell TPh21.
These different values of pressure are due to the different value of relative permanent displacement recorded at wall top and base. This first stage is generated by the inertial forces that occur near the top of the wall due to the failure wedge shape. Whereas the acceleration level was increasing together to the permanent rotation at the top of the wall, the threshold acceleration was reached and a base displacement was clearly evident. At this stage the pressures change and the system involved in a rotation about the top mode. The pressures measured by cells TPh3 and TPh9 began to build up with small rotation angles. A soil arching developed in the backfill and a new dynamic pressure distribution appeared, totally different from the previous one. This difference results in a higher point of application of the total thrust. When the soil-wall friction was reduced the soil arching effect maintained constant since low levels of acceleration, and the pressure distribution was strongly influenced. The passive phenomena observed during the test near the top, where large vibration were recorded, are due to different modes of vibration for the wall and the backfill, especially when the soil degradation and the effects of strain localization and post-peak reduction in shear resistance occur in the backfill soil generating a reduction in the natural frequency of the soil-structure system. The tests performed show that a strong reduction of soil-wall friction produces a distribution of total dynamic pressure with a point of application placed near the top of the wall and with a value that differ from the M&O prediction. This aspect is evident also during the tests without reduction of soil-wall friction angle, where the recorded values of pressure at the two failure stages are always higher than those estimated by Mononobe-Okabe's formula. When the acceleration level was increased and the failure of the system was due to a rotational about top mode, the soil wedge formed tends to push up the wall, because a change for an upward shear force was occur. The failure surface shape shows the concavity toward the backfill. When the soil-wall friction angle was reduced a similar behaviour did not appear and a plane failure surface formed with a smaller failure wedge. The previous discussions shows that a low value of soil-wall friction angle produces a strong increment of the acceleration amplification near the top of the wall, generating a non-linear pressures distribution with an higher point of application. The soil-wall friction reduction produce a reduction of the amplification of wall top acceleration. Moreover for all the tests conducted, it was observed that the reduction of soil-wall friction produce large deformation also into the backfill outside the failure wedge.

CONCLUSIONS

The following conclusions could be made based on the experimental results obtained and discussed in this paper:

- The dynamic pressure distribution is strongly influenced by the wall movement modes and two different stages were observed during the same test;
- An "elastic" displacement is exerted by the wall during the initial stage of the motion producing a sort of reduction in the acceleration amplification;
- a reduction of soil-wall friction angle produces a large increment of acceleration level at the wall top;
- for rotation about base mode, that occur during the first stage, the dynamic earth pressure distribution is non-linear with depth and the point of application is near the base of the wall;

- For rotation about top, during the second stage, the dynamic pressure distribution is non linear with depth, arching soil stress was deduced acting near the top of the wall and higher point of application of the resultant is reached;
- a strong reduction of soil-wall friction angle produces a distribution of total dynamic pressure with a point of application placed near the top of the wall and with a value that differ from the M&O prediction;
- Failure wedge shape is influenced by soil-wall friction angle deducing a change in the inertia forces;
- All the experimental values of dynamic pressures measured, are higher respect to the theoretical values of the active earth equations given by Mononobe & Okabe. This indicates a "passive" state due to relative displacements of soil-wall system, especially near the top of the wall..

REFERENCES

1. V. S. Fang, I. Ishibashi, "Static Earth Pressure with Various Wall Movements", Journal of Geotechnical Engineering, ASCE, Vol. 112, N. 3, 1986.
2. Ishibashi, V. S. Fang "Dynamic Earth Pressures with Different Wall Movement Modes", Soils and Foundations, Vol. - 27, N. 4, 1987.
3. A. S. Lo Grasso, "Experimental dynamic analysis of the earth pressure distribution on a gravity retaining wall by shaking table tests", Ph.D. Dissertation, Geotechnical Engineering, University of Catania, Italy, December 2002.
4. H. Matsuo, S. Ohara, "Lateral Earth Pressures and Stability of Quay Walls during Earthquakes", Proc. 2nd World Conference on Earthquake Engineering, Tokyo, Japan, 1960.
5. N. Mononobe, R. Matsuo, "On the Determination of Earth Pressure during Earthquake", Paper No. 388, Proc. of World Engineering Congress, Vol. 9, 1929.
6. P. Nandakumaran, V. H. Joshi, "Static and dynamic Active Earth Pressure behind Retaining Walls", Bulletin of the Indian Society of Earthquake Technology, Vol, 10, N. 3, September 1973
7. P. Nandakumaran, V. S. Prasad, "Experimental Determination of Dynamic Passive Pressure of sand", Proc., 7th World Conference on Earthquake Engineering, Istanbul, Turkey, 1980.
8. S. Okabe, "General Theory of Earth Pressure", Journal of Japanese Society of Civil Engineers, Vol. 12, N. 1, 1926.
9. M. A. Sherif, Y. S. Fang, "Dynamic Earth Pressures on Walls Rotating About Top", Soil and Foundation, Vol. 24, N.4m 1994.
10. M. A. Sherif, I. Ishibashi, C. D. Lee, "Earth Pressures against Rigid Retaining Walls", Journal of Geotechnical Engineering, ASCE, Vol. 108, 1982.
11. A. H. Soubra, B. Macuh, "Seismic Active and Passive Earth Pressure on Rigid Retaining Structures by a Kinematical Approach", 4th International Conference on Recent Advances in Geotechnical Earthquake engineering and Soil Dynamics and Symposium in Honour of Professor W.D. Liam Finn, San Diego California, March 2001.
12. R. S. Steedman, X. Zeng, "The Influence of Phase on the Calculation of Pseudo-static Earth Pressure on a Retaining Wall", Geotechnique, 40, n.1,1990.
13. J. M. Zhang, Y. Shamoto, K. Tokimatsu, "Earth Pressure on Rigid Walls During Earthquake", Geotechnical Earthquake Engineering and Soil Dynamics III, ASCE 1998.
14. J. M. Zhang, Y. Shamoto, K. Tokimatsu, Seismic Earth Pressure theory for Retaining Walls Under Any Lateral Displacements, Soil and Foundations, Vol.38, N.2, 1998
15. J. M. Zhang, Y. Shamoto, K. Tokimatsu, Evaluation of Earth Pressure Under Any Lateral Deformation, Soil and Foundations, Vol.38, N.1, 1998
16. J. M. Zhang, D. Li "Seismic Active Earth Pressure Considering Effect of Strain Localization", 4th International Conference on Recent Advances in Geotechnical Earthquake engineering and Soil Dynamics and Symposium in honor of Professor W.D. Liam Finn, San Diego California, March 2001.